Interaction of a Compressible Bubbly Flow With an Obstacle Placed Within a Shedding Partial Cavity

Harish Ganesh, Simo A Mäkiharju, Steven L. Ceccio

University of Michigan, Ann Arbor, MI 48109, USA

E-mail: gharish@umich.edu

Abstract. Bubbly shocks act as the dominant mechanism of shedding of partial cavities under certain conditions. The compressible nature of low void fraction regions in a partial cavity can provide conditions necessary for the existence of such bubbly shocks. Using X-ray densitometry as a flow visualisation mechanism, the dynamics of bubbly shock fronts with and without the presence of an obstacle are presented. Different flow features associated with the shock dynamics are identified and the associated flow physics explained.

1. Introduction

Hydrodynamic cavitation can occur in separated regions of flow behind objects resulting in partially filled vapor cavities. Once formed, partial cavities are generally stable, but can experience auto oscillations of cavity length resulting in shedding of vapor clouds, termed as cloud cavitation, carrying the vapor filled mixture that originally formed the cavity. Cloud cavitation and its onset are detrimental, and it is one of the principal agents of cavitation erosion. Measured values of void fraction in a partial cavity, as discussed in [1], [2], [3] and [4, 5] suggest that the cavity is not very dense under certain conditions. This means that the local speed of sound in such scenarios can be very small resulting in high local Mach numbers. A discussion of variation of speed of sound with void fraction can be found in [6]. Low values of speed of sound results in smaller propagation speed of disturbances than in liquids and lead to the presence of strong shock waves. [4] discusses the role of bubbly shocks in the shedding of partial cavities on a wedge and their relationship to the underlying cavitating flow field. The present study deals with the interaction of such propagating bubbly shocks with solid obstacles placed on the geometry used [4, 5]. Using X-ray densitometry as a flow visualization technique, the dynamics of the bubbly shock wave with and without an obstacle are studied. Different types of wave interactions that suggest the presence of complex flow physics involved are presented.

2. Experimental Setup

Experiments were carried out at the University of Michigan 9-Inch Water Tunnel. The tunnel has a 6:1 round contraction leading into a test section with a diameter of 23 cm (9 inches). The test section then transitions to a square cross-section that is 21 cm by 21 cm with chamfered corners. The flow velocity in the tunnel test section can be varied from $U_0 = 0$ to 18 m/s and the static pressure, p_0, from near vacuum to 200 kPa.

$$\sigma_0 = \frac{(p_0 - p_v)}{\frac{1}{2}\rho U_0^2} \quad (1)$$

In the present experiments, the test section was further reduced in area to a conduit that had a 7.6 cm by 7.6 cm cross-section. This was done to reduce the baseline X-ray attenuation produced by the non-cavitating flow. The wedge geometry was chosen because it produces a nominally two-dimensional cavity with a well-defined line of cavity detachment. The wedge makes an angle of 22.1 degrees to the incoming flow, and has a downstream angle of 8.1 degrees. [4, 5] discuss the set-up and geometry in more detail. A schematic of the wedge in the test section is shown in Figure 1.

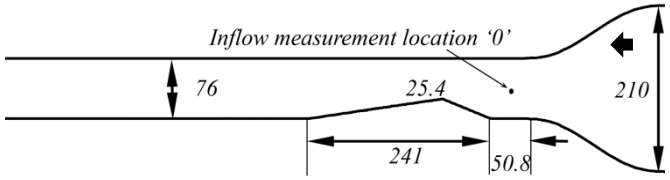

Figure 1: Schematic of the wedge (without the obstacle) in the test section. All dimensions are in 'mm'.

X-ray densitometry is based on the principle of Beer-Lambert's law of attenuation of ionizing radiation. The X-ray densitometry system used in the present study had a source capable of 433 mA at 150 kV, and the imaging system is comprised of an image intensifier coupled with a high-speed camera (Vision Research Phantom V9.0). By shooting an X-ray beam into the partial cavity with vapor, the void fraction flow field can be determined by analyzing the attenuated image of the cavity. From the void fraction field, one can track interfaces such as shock waves, cavities, and shed vapor clouds. A detailed description of the method can be found in [7].

3. Shedding Partial Cavity

The wedge geometry provides conditions for sustainable cavitation at the wedge apex. By systematically changing the inlet pressure p_0, the inlet cavitation number was varied to study different types of cavities. At higher cavitation numbers ($\sigma_0 > 2.2$), the cavities at the wedge apex were relatively stable and with reduction in inlet cavitation number, σ_0, the cavities began to exhibit significant length oscillations. When the inlet cavitation number was decreased to $\sigma_0 < 1.9$ +/-0.1, periodically shedding cavities were observed.

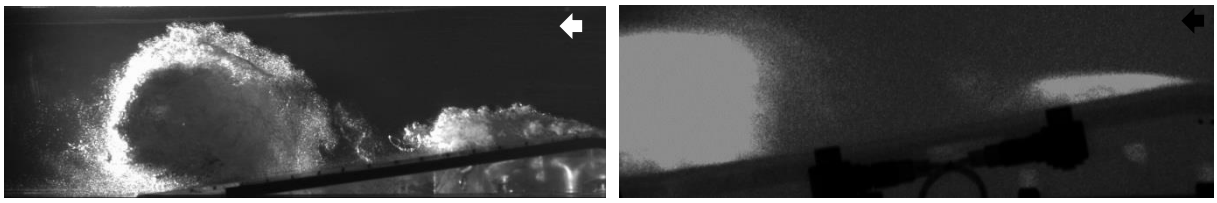

(a) (b)

Figure 2: A shedding cavity at $U_0 = 8$ m/s (a) High speed video image at $\sigma_0 = 1.85$ +/-0.1 (b) X-ray attenuation field image at $\sigma_0 = 1.81$ +/-0.1.

Figure 2(a) shows a snapshot of a periodically shedding cavity using high speed video. The X-ray densitometry snapshot image for periodically shedding cavity is shown in Figure 2(b). From the images, flow features like cavity closure and shed vapor cloud can be clearly seen. Figure 3 shows a time series of a shedding cavity with the associated flow features. The cycle has well defined growth and pinch-off with the propagating shock from clearly visible in Figures 3(c) and 3(d).

4. Interaction of shock wave with obstacle

A small obstacle of cross-sectional size 4mm x 4mm that spanned the wedge was placed with its leading edge 63mm from the wedge apex.

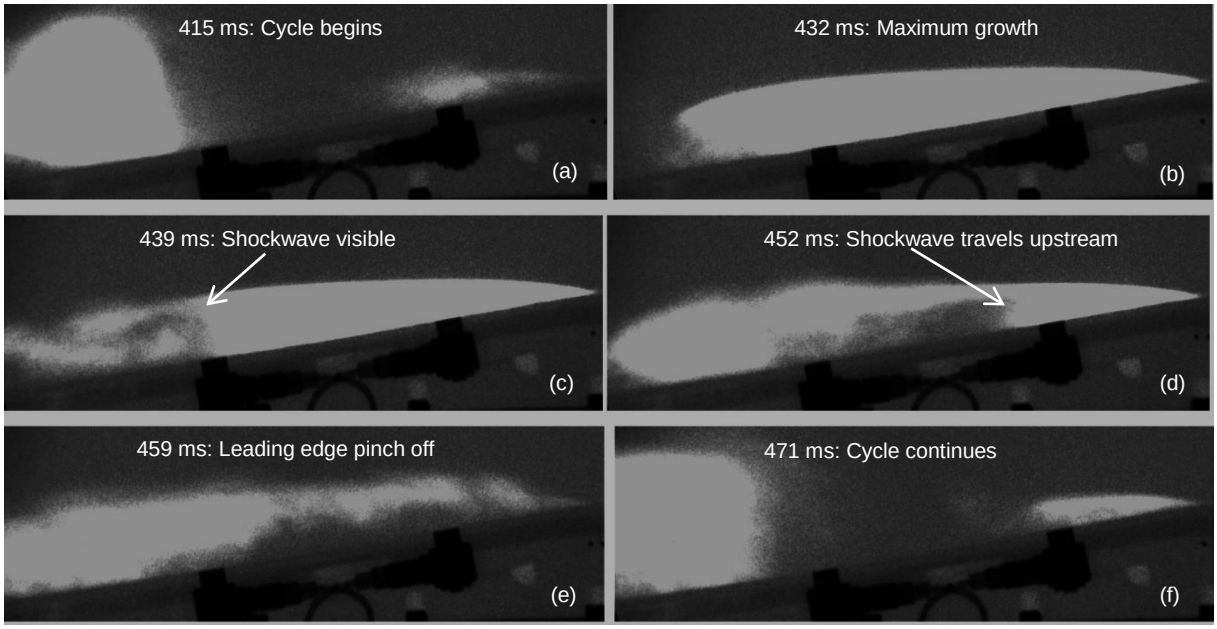

Figure 3: Time series of X-ray images showing a shedding cavity cycle at U_0 = 8 m/s and σ_0 =1.85 +/- 0.1. In this case, no obstacle is present.

Time resolved X-ray attenuation videos were recorded to study the interaction of the shock wave with the obstacle as shown in Figures 4, 5 and 6. As the cavity grows, the void fraction in the cavity reduces resulting in low speed of sound values. Speed of sound for this particular flow is found to be around 3 to 5m/s [4, 5]. Once the cavity length crosses the obstacle the effect of low speed of sound is felt locally. Since the obstacle is in the region of recirculation, an oblique shock wave forms to aid the recirculating flow to cross the obstacle. This is different from the propagating normal shock wave that results in shedding. This is shown in Figure 4(a) and 4(b). Figure 4(b) also shows the interaction of the oblique shock wave with the expansion fan that exists in the cavity. It should be noted that this expansion is a result of the propagating shock being reflection back as an expansion from the wedge apex.

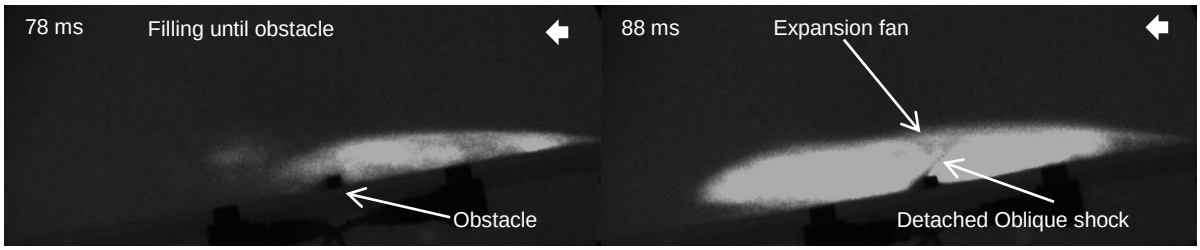

Figure 4: Cavity dynamics in the presence of an obstacle in filling phase of the cycle for U_0 = 8 m/s and σ_0 =1.85 +/-0.1

Figures 5(a) and (b) show the interaction of the normal shock wave with the obstacle. Once the normal shock wave crosses the obstacle, the wake of the obstacle is filled with vapour. This could be due to the cavitation of the re-entering liquid drawn by the shock as it moves into a vapour filled cavity or due to the rarefactions waves produced by the passage of shock over a sharp edge. The recirculation zone present at the aft of the obstacle transitions into a stagnation mass of bubbly fluid once the void fraction values drop below a certain value. This results in the disappearance of the oblique shock (that was seen in 4b) because of the absence of the re-entrant flow.

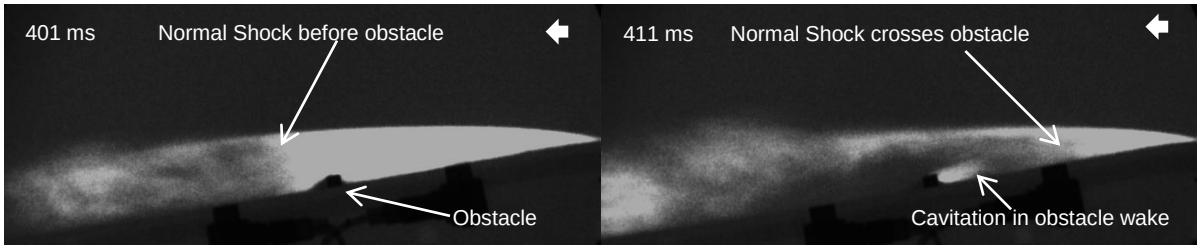

*Figure 5: Cavity dynamics in the presence of an obstacle in collapse phase of the shedding cycle for U_0 = 8 m/s and σ_0 =*1.85 +/-0.1

For smaller cavity lengths and higher cavitation number, the interaction of the stationary oblique shock and the propagating normal shock is feasible. One such interaction is shown in Figure 6(a) and 6(b). For this case the cavity length was such that the detached shock occurrence due to changes in void fraction values near the obstacle and the initiation of a propagating bubbly shock occurred very close to each other in time. This can be visualised in Figures 6(b) where the complex interaction of the shock waves and the expansion fans can be seen. More information on the kind of interactions between the waves can be found in [8].

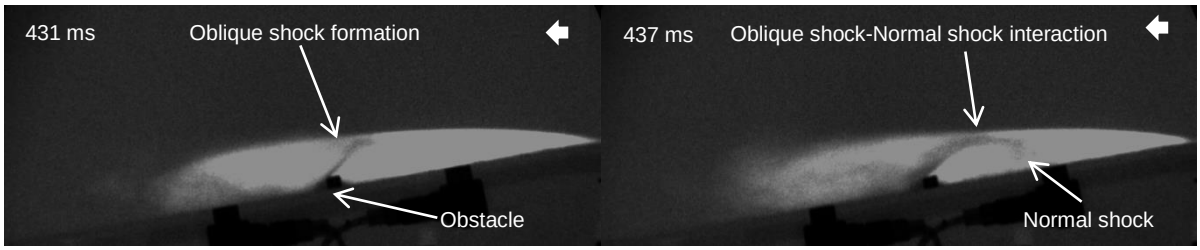

*Figure 6: Shock-Shock Interaction U_0 = 8 m/s and σ_0 =*1.94 +/-0.1

References

[1] Coutier-Delgosha, O., Stutz, B., Vabre, V. & Legoupil, S. (2007) Analysis of cavitating flow structure by experimental and numerical investigations. *J. Fluid Mech.* **578**, 171-222

[2] Stutz, B & Reboud, J. L. (1997a) Experiements on unsteady cavitation. *Expt in Fluids.* **22**, 191-198Stutz, B & Reboud, J. L. (1997b) Two-phase flow structure of sheet cavitation. *Physics of fluids.* **9**, 12, 3678-3686.

[3] Stutz, B & Legoupil, S. (2003) X-ray measurements within unsteady cavitation. *Expt in Fluids.* **35**, 130-138

[4] Ganesh, H., Mäkiharju, S.A**.**, & Ceccio, S.L. (2015) Bubbly shock propagation as a mechanism for sheet-to-cloud transition of partial cavities. *J. Fluid Mech.* (Submitted)

[5] Ganesh, H. (2015) Bubbly shock propagation as a cause of sheet to cloud transition of partial cavitation and stationary cavitation bubbles forming on a Delta wing vortex. *Ph.D Thesis, University of Michigan*

[6] Brennen, C, E. (2005) "Fundamentals of multiphase flows", *Cambridge University Press*

[7] Mäkiharju, S.A**.**, Chang, N., Gabillet, C., Paik, B.-G., Perlin, M. & Ceccio, S.L. (2013) Time Resolved Two Dimensional X-Ray Densitometry of a Two Phase Flow Downstream of a Ventilated Cavity. *Experiments in Fluids*, **54**,

[8] Liepmann, H., W., & Roshko, A. (2001) "Elements of Gas Dynamics", *Dover Publications*